Metal Nanoparticles

International Edition: DOI: 10.1002/anie.201503269
German Edition: DOI: 10.1002/ange.201503269

Sodium-Naphthalenide-Driven Synthesis of Base-Metal Nanoparticles and Follow-up Reactions**

*Christian Schöttle, Pascal Bockstaller, Radian Popescu, Dagmar Gerthsen, and Claus Feldmann**

Dedicated to Professor Manfred Scheer on the occasion of his 60th birthday

Abstract: *Mo^0, W^0, Fe^0, Ru^0, Re^0, and Zn^0 nanoparticles—essentially base metals—are prepared as a general strategy by a sodium naphthalenide ([NaNaph])-driven reduction of simple metal chlorides in ethers (1,2-dimethoxyethane (DME), tetrahydrofuran (THF)). All the nanoparticles have diameters ≤ 10 nm, and they can be obtained either as powder samples or long-term stable suspensions. Direct follow-up reactions (e.g., $Mo^0 + S_8$, $FeCl_3 + AsCl_3$, $ReCl_5 + MoCl_5$), moreover, allow the preparation of MoS_2, $FeAs_2$, or Re_4Mo nanoparticles of similar size as the pristine metals (≤ 10 nm).*

Metal nanoparticles are of fundamental interest in view of basic chemistry (e.g., quantum-confinement effects, manipulation of structure and shape) and application (e.g., catalysis, thin-film electronics, high-power batteries, solar cells).[1] Today, the structure and shape especially of precious-metal nanoparticles (e.g. Pd, Pt, Ag, Au) can be controlled and manipulated with fascinating virtuosity.[1a,d,2] Owing to the dramatically increased reactivity (including re-oxidation and hydrolysis), however, chemical synthesis of base-metal nanoparticles becomes the more challenging the smaller the particles are and the less-noble the respective metal is. Therefore, access to high-quality nanoparticles of base metals is still limited.

In view of the starting materials, liquid-phase synthesis of base-metal nanoparticles has been conducted via the decomposition of low-valence metal precursors (e.g., carbonyl, alkyl, aryl complexes) or the reduction of metal salts (e.g., halides, alkoxides).[1–3] Of these, volatile and toxic carbonyl metals have been most widely used, especially, for preparing nanoscaled Mo^0, W^0, Fe^0, or Re^0 particles.[3,4] High-boiling and/or strongly coordinating solvents (e.g., long-chained alkylamines or alkylthiols, ionic liquids) are typically needed to control particle size, particle growth, and agglomeration.[1–3] Practical aspects of synthesis have to ensure the exclusion of oxygen and moisture, the colloidal stabilization of the reactive metal nanoparticles right after nucleation as well as the separation and purification of the nanoparticles after synthesis.

As strong reducing agents, H_2, $NaBH_4$, $(SiMe_2)_6$, Mg, or Na^0 in liquid NH_3 have been used under partly harsh conditions.[5] However, particle size and agglomeration are often hard to control, and oxide impurities are difficult to avoid. Access to Zn^0 nanoparticles, for instance, is dominated by gas-phase deposition and limited to a few liquid-phase methods, using organozinc compounds or electrodeposition.[6] Generally the synthesis of reactive, base-metal nanoparticles with uniform small size (≤ 10 nm) and low agglomeration is still a challenge, so that alternative synthesis strategies—preferentially based on low-cost and easy-to-handle starting materials, reducing agents, and solvents—are highly requested.

Herein, we report on the liquid-phase synthesis of Mo^0, W^0, Fe^0, Ru^0, Re^0, and Zn^0 nanoparticles with diameters of no more than 10 nm. Simple metal chlorides are used as starting materials and reduced by sodium naphthalenide ([NaNaph]) in 1,2-dimethoxyethane (DME) or tetrahydrofuran (THF; Figure 1). It is to be noted that controlling particle size and agglomeration does not require any additional agent for surface functionalization and colloidal stabilization. The reactive metal nanoparticles can be easily obtained with yields of 95–99% either as powder samples or as long-term stable colloidal suspensions. Moreover, the metal nanoparticles can be readily reacted to give other metal nanoparticles. This is shown for MoS_2, $FeAs_2$, and Re_4Mo nanoparticles which are produced in the same size range (≤ 10 nm) as the pristine metal nanoparticles (Figure 1).

[NaNaph] is a strong reducing agent used in inorganic synthesis, for instance, to establish B–B triple bonds or to obtain low-valence silicon, germanium, or transition-metal compounds.[7] [NaNaph] has been reported to be an even more powerful reducing agent than sodium (E_0(Na/liquid NH_3) = −2.3 V, E_0([NaNaph]/THF) = −3.1 V).[8] It can be easily prepared by treating sodium metal with naphthalene in absolute ethers, such as DME or THF. The resulting deep green solution is stable for weeks (under argon), easy to portion with a syringe (in contrast to solid sodium metal), and can be handled at ambient pressure and temperature (in contrast to liquid ammonia). As the injection of a homogenously dissolved strong reducing agent is optimal for control-

[*] Dipl.-Chem. C. Schöttle, Prof. Dr. C. Feldmann
Institut für Anorganische Chemie
Karlsruhe Institute of Technology (KIT)
Engesserstrasse 15, 76131 Karlsruhe (Germany)
E-mail: claus.feldmann@kit.edu
Dr. P. Bockstaller, Dr. R. Popescu, Prof. Dr. D. Gerthsen
Laboratorium für Elektronenmikroskopie
Karlsruhe Institute of Technology (KIT)
Engesserstrasse 7, 76131 Karlsruhe (Germany)

[**] We are grateful Dr. R. Schneider, KIT, for performing EELS analysis. We thank the Deutsche Forschungsgemeinschaft (DFG) for funding (NanoMet: FE911/4-1, GE 841/22-1, SPP1708 "Synthesis near room temperature"). Finally, C.S. acknowledges the Karlsruhe Graduate School of Optics and Photonics (KSOP) for scholarship.

Supporting information for this article is available on the WWW under http://dx.doi.org/10.1002/anie.201503269.

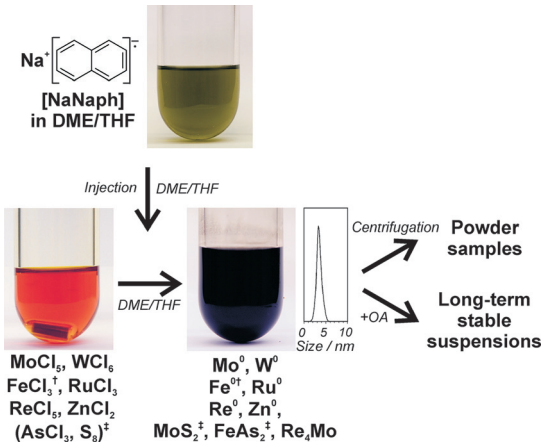

Figure 1. Scheme illustrating the synthesis of Mo^0, W^0, Fe^0, Ru^0, Re^0 and Zn^0 nanoparticles by reduction of metal chlorides with sodium naphthalenide ([NaNaph]) in ether (1,2-dimethoxyethane (DME) or tetrahydrofuran (THF)) as well as follow-up reactions to obtain MoS_2, $FeAs_2$, and Re_4Mo nanoparticles (†Photos and size distribution for the reduction of $FeCl_3$ to Fe^0 nanoparticles; ‡Addition of S_8 and $AsCl_3$ to obtain MoS_2 and $FeAs_2$; OA: oleylamine; see Experimental Section for details).

Table 1: Starting materials, mean particle diameters, and lattice distances of the as-prepared Mo^0, W^0, Fe^0, Ru^0, Re^0, and Zn^0 nanoparticles.

Metal	Starting material	Mean particle diameter [nm][a]	Lattice distance [Å]
Mo^0	$MoCl_5$	1.5 ± 0.4	non-crystalline
W^0	WCl_6	1.1 ± 0.3	non-crystalline
Fe^0	$FeCl_3$	3.4 ± 0.5	2.0 (110)
Ru^0	$RuCl_3$	2.0 ± 0.6	2.0 (101), 2.3 (100)
Re^0	$ReCl_5$	1.1 ± 0.2	2.4 (100)
Zn^0	$ZnCl_2$	10.1 ± 2.3	2.1 (101)

[a] Mean diameters from statistical evaluation of TEM images (Figure S1).

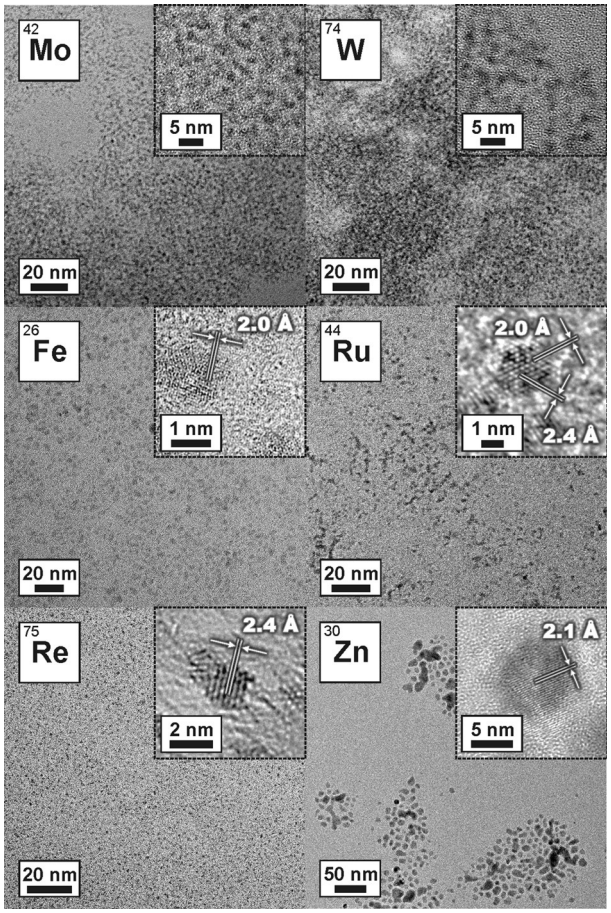

Figure 2. TEM overview and detail images (inset) of the as-prepared Mo^0, W^0, Fe^0, Ru^0, Re^0, and Zn^0 nanoparticles (see Supporting Information for DLS, STEM, FT-IR, XRD).

ling nucleation and growth of nanoparticles, solutions of [NaNaph] are ideal for obtaining small-sized, base-metal nanoparticles. Thus, it is surprising that to date [NaNaph] has rarely been used for preparing nanoparticles. In this way, the main-group elements boron, silicon, and germanium have been obtained on the nanoscale employing long-chained alcohols as stabilizing agents to control particle size and agglomeration.[9] Moreover, bimetallic platinum and gold nanoparticles have been obtained by [NaNaph]-driven reduction.[10] Recently, poly(methyl methacrylate)-coated magnesium nanoparticles were obtained by [LiNaph]-driven reduction of $[Mg(Cp)_2]$ ($Cp = C_5H_5$) and used for hydrogen storage.[11] In this case, the polymer coating was needed to suppress hydrolysis/oxidation of Mg^0, but it also limits the H_2 uptake.

We obtained Mo^0, W^0, Fe^0, Ru^0, Re^0, and Zn^0 nanoparticles by reduction of less-expensive, commercially available metal chlorides (i.e., $MoCl_5$, WCl_6, $FeCl_3$, $RuCl_3$, $ReCl_5$, $ZnCl_2$) by the injection of [NaNaph] as a strong reducing agent in DME or THF (Table 1, Figure 2). DME or THF were used to guarantee optimal solubility of the chloride precursors. After injection of [NaNaph] into the DME or THF solutions of the metal chlorides, the formation of metal nanoparticles is indicated by instantaneous formation of black suspensions. These DME or THF suspensions are colloidally stable for several hours. From the as-prepared suspensions, the metal nanoparticles can be separated by centrifugation to obtain powder samples with yields of 95–99% (Figure 1, and Supporting Information, Figure S1). Alternatively, long-term stable suspensions (up to months) can be obtained upon post-synthesis addition of oleylamine (Figure 1, and Figure S2). Thereafter, even high-power centrifugation (up to $50000 \times g$) does not lead to any precipitation (Figure S3). Separation of the post-synthesis oleylamine-stabilized metal nanoparticles is possible by hydrazine treatment (Figures S4,S5).[12] It is to be noted that oleylamine is absent during particle nucleation and only needed for long-term stabilization. Except for Ru^0, all the small-sized, base metals are highly reactive and need to be handled under inert conditions (N_2, Ar, vacuum). Contact to air and/or moisture can lead to instantaneous oxidation, partially occurring with combustion (especially, in the case of Mo^0, W^0, Fe^0, Zn^0).

Transmission electron microscopy (TEM) overview and detail images show non-agglomerated nanoparticles of the as-prepared Mo^0, W^0, Fe^0, Ru^0, Re^0 and Zn^0 with narrow size distribution and mean particle diameters less than or equal to

10 nm (Table 1, Figure 2, Figures S2,S5–S14). Immediately after synthesis, Fe^0, Ru^0, Re^0, and Zn^0 were crystalline and show lattice fringes on HRTEM images (Figure 2). The observed distances are well in agreement with the respective bulk references: Fe^0 with 2.0 Å (bulk-Fe^0: $d_{110} = 2.027$ Å); Ru^0 with 2.0 and 2.3 Å (bulk-Ru^0: $d_{101} = 2.056$ Å, $d_{100} = 2.343$ Å); Re^0 with 2.4 Å (bulk-Re^0: $d_{100} = 2.388$ Å); Zn^0 with 2.1 Å (bulk-Zn^0: $d_{101} = 2.091$ Å). HRTEM images of as-prepared Mo^0 and W^0 do not show any lattice fringes, which can be attributed to low diffusion in the solid state since both are hard metals with high melting points (> 2500 °C). In addition to TEM analysis, the purity of all the as-prepared metal nanoparticles is confirmed by X-ray powder diffraction (XRD) after powder sintering (≥ 800 °C, Ar). Although non-nanoparticulate thereafter, the presence of the respective metal and, especially, the absence of oxide impurities is clearly confirmed (Figure S6).

Besides the synthesis of base-metal nanoparticles by [NaNaph]-driven reduction, we have considered their use as reactive precursors for obtaining metal compounds (such as chalcogenides, alloys, intermetallic compounds, Zintl phases). Such options further enhance the applicability of the synthesis strategy. From the number of feasible compounds, we have representatively selected MoS_2, $FeAs_2$, and Re_4Mo (Figures 1,3). Of these, nanoscaled MoS_2 recently became highly relevant for photocatalytical hydrogen generation, multilayer transistors, and lithium-ion storage.[13] FeX_2 derivatives (X: As, Sb) are discussed as nanostructured superconductors ($FeAs_2$) and thermoelectrics ($FeSb_2$).[14] Re_4Mo has been selected in view of it use in nanoscaled catalysts.[15]

MoS_2 nanoparticles—our first example—were obtained by treating the as-prepared Mo^0 nanoparticles with a solution of sulfur in toluene (Figure 1). After reaction (110 °C, 2 h), a slight increase in particle size (MoS_2: 1.7 ± 0.5 nm) was observed in the TEM and high-angle annular dark-field scanning transmission electron microscopy (HAADF-STEM) images (Figure 3; Figure S15) in comparison to the pristine Mo^0 (1.5 ± 0.4 nm; Figure 2). Energy-dispersive X-ray spectroscopy (EDXS) and electron energy loss spectroscopy (EELS) show the presence of molybdenum (*K*-, *L*-lines) and sulfur (*K*-, *L*-lines; Figure 3; Figure S16). Detailed analysis of EDXS peak intensities gave a Mo:S ratio of 35:65 fitting well with MoS_2 (Figure S15). Since the as-prepared MoS_2 is amorphous, sintering (1000 °C, vacuum) was used for complete crystallization. Although agglomerated, XRD thereafter clearly shows the presence of MoS_2 and the absence of impurity phases (e.g., Mo^0, MoO_x) (Figure S6). Moreover, complete reaction of Mo^0 to MoS_2 is indicated by thermogravimetry (TG), showing that almost no excess sulfur remains (excess $S_8 \leq 2\%$, Figure S17).

$FeAs_2$ nanoparticles were obtained by co-reduction of $FeCl_3$ and $AsCl_3$ with [NaNaph] (Figure 1). Again, TEM and HAADF-STEM images show uniform, non-agglomerated particles with a mean diameter of 2.9 ± 0.5 nm (Figure 3; Figure S18). EDXS area scans verify the presence of iron (*K*-, *L*-lines) and arsine (*K*-, *L*-lines; Figure 3; Figure S19; the additional Cu K-lines stem from the copper-grid sample holder (see Supporting Information)). The Fe:As ratio was determined to 1.0:2.1. Since the as-prepared $FeAs_2$ is amorphous, sintering (500 °C, Ar) was used to confirm the phase purity of $FeAs_2$ and the absence of impurity phases (e.g., Fe^0, As^0, Fe_xO_y, As_xO_y) by XRD (Figure S6).

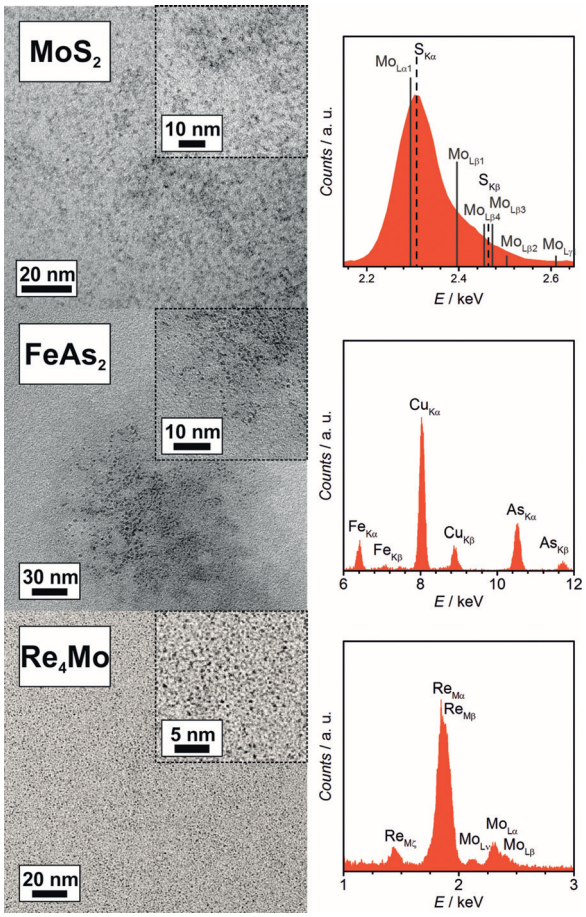

Figure 3. TEM overview and detail images (inset) as well as EDXS of MoS_2, $FeAs_2$, and Re_4Mo nanoparticles (see Supporting Information for STEM, XRD, FT-IR, EELS, TG).

Co-reduction of $ReCl_5$ and $MoCl_5$ with [NaNaph] results in bimetallic Re_4Mo nanoparticles (Figure 1). TEM and HAADF-STEM images reveal non-agglomerated, uniform nanoparticles with a mean diameter of 1.1 ± 0.2 nm (Figure 3; Figure S20). EDXS confirms the presence of molybdenum (*K*-, *L*-lines) and rhenium (*L*-, *M*-lines) (Figure 3; Figure S21). The Re:Mo ratio was determined to 4.4:1.0. Owing to the very small particle diameter, EDXS line scans or mappings were not significant. Therefore, EDXS spot measurements were performed and confirmed the Re:Mo ratio for some ten nanoparticles. Again, the as-prepared nanoparticles are amorphous. After sintering (1000 °C, Ar), XRD confirms the presence of Re_4Mo and the absence of impurity phases, such as Re^0, Mo^0, or eventual oxides (Figure S6).[16]

In conclusion, a range of reactive, base-metal nanoparticles was prepared, including Mo^0, W^0, Fe^0, Ru^0, Re^0, and Zn^0. Using low-cost metal chlorides as the starting materials and [NaNaph] as a strong reducing agent facilitates the reaction and allows for straightforward liquid-phase synthesis. The reaction was performed in ethers (DME, THF) without

any additional stabilizing agent for controlling particle nucleation, particle growth, and agglomeration. After the synthesis, alternatively, powder samples (by direct centrifugation) or long-term stable suspensions (upon post-synthesis addition of oleylamine) are obtainable. The reactive metal nanoparticles can be directly transformed to metal nanoparticle compounds, such as MoS_2, $FeAs_2$, and Re_4Mo exhibiting similar diameters as the pristine metal nanoparticles. In future, this concept of synthesis may become a general and reliable strategy for obtaining a tool-box of nanoscaled base metals and metal nanoparticle compounds thereof with applications ranging from catalysis, magnetic and hard materials, to batteries and solar cells.

Experimental Section

Sodium naphthalenide ([NaNaph]): Sodium metal (46.0 mg, 2.0 mmol) was dissolved in a solution of naphthalene (270.0 mg, 2.1 mmol) in 1,2-dimethoxyethane (DME, 5.0 mL) or tetrahydrofuran (THF, 5.0 mL) over 12 h. DME or THF were used depending on the solubility of the respective metal chloride.

Mo^0 nanoparticles: $MoCl_5$ (109.3 mg, 0.4 mmol) was dissolved in DME (15 mL). After injection of [NaNaph] in DME, the red solution turned black immediately. Thereafter, the suspension can be centrifuged to obtain Mo^0 powder samples. The nanoparticles were twice redispersed/centrifuged in/from absolute methanol to remove all chlorides, and dried in vacuum. Optional sintering of powders was conducted at 900 °C, 1 h in hydrogen.

To obtain long-term stable suspensions (up to months), the Mo^0 nanoparticles can be redispersed in *n*-heptane, containing oleylamine (OA, 2.0 mL, 6.08 mmol). From these post-synthesis OA-stabilized suspensions, the nanoparticles can be separated in turn after destabilization upon addition of hydrazine in THF (4.0 mL, 1.0 M).[12]

W^0, Fe^0, Ru^0, Re^0, and Zn^0 nanoparticles were prepared similar to the Mo^0 nanoparticles (see Supporting Information for detailed information).

MoS_2 nanoparticles: $MoCl_5$ (109.3 mg, 0.4 mmol) was dissolved in DME (15 mL). After injection of [NaNaph] in DME, the red solution turned black immediately. The obtained Mo^0 nanoparticles were centrifuged and redispersed in absolute toluene. Next, a solution of sulfur (25.6 mg, 0.8 mmol) and oleylamine (2.0 mL, 6.08 mmol) in toluene (20 mL) was added. Thereafter, the suspension was refluxed for 3 h and subsequently destabilized by adding hydrazine in THF (4.0 mL, 1.0 M). The MoS_2 nanoparticles were separated by centrifugation and washed twice with methanol (25 mL). Optional sintering of powder samples was performed by sintering at 1000 °C for 7 h in vacuum.

$FeAs_2$ nanoparticles: $FeCl_3$ (54.1 mg, 0.33 mmol) and $AsCl_3$ (0.03 mL, 64.8 mg, 0.36 mmol) were dissolved in DME (15 mL). After injection of [NaNaph] in DME, the yellow solution turned black immediately. Powder samples and long-term stabilized suspensions were obtained as described for Mo^0. Optional sintering of powder samples was performed by sintering at 500 °C for 7 h in vacuum.

Re_4Mo nanoparticles: $ReCl_5$ (116.3 mg, 0.32 mmol) and $MoCl_5$ (21.9 mg, 0.08 mmol) were dissolved in DME (15 mL). After injection of [NaNaph] in DME, the red solution turned black immediately. Powder samples and long-term stabilized suspensions were obtained as described for Mo^0. Optional sintering of powder samples was performed by sintering at 1000 °C for 7 h in an argon atmosphere.

Further details regarding synthesis and characterization of the nano-particles can be obtained from the Supporting Information.

Keywords: base metals · nanoparticles · sodium naphthalenide · synthetic methods

How to cite: *Angew. Chem. Int. Ed.* **2015**, *54*, 9866–9870
Angew. Chem. **2015**, *127*, 10004–10008

[1] Reviews: a) H. You, S. Yang, B. Ding, H. Yang, *Chem. Soc. Rev.* **2013**, *42*, 2880; b) H. Goesmann, C. Feldmann, *Angew. Chem. Int. Ed.* **2010**, *49*, 1362; *Angew. Chem.* **2010**, *122*, 1402; c) T. K. Sau, A. L. Rogach, F. Jäckel, T. A. Klar, J. Feldmann, *Adv. Mater.* **2010**, *22*, 1805; d) C. Burda, X. Chen, R. Narayanan, M. A. El-Sayed, *Chem. Rev.* **2005**, *105*, 1025.

[2] Reviews: a) M. R. Buck, R. E. Schaak, *Angew. Chem. Int. Ed.* **2013**, *52*, 6154; *Angew. Chem.* **2013**, *125*, 6270; b) Y. Lu, W. Chen, *Chem. Soc. Rev.* **2012**, *41*, 3594; c) B. Lim, Y. Xia, *Angew. Chem. Int. Ed.* **2011**, *50*, 76; *Angew. Chem.* **2011**, *123*, 78; d) T. K. Sau, A. L. Rogach, *Adv. Mater.* **2010**, *22*, 1781.

[3] Reviews: a) S. Mourdikoudis, L. M. Liz-Marzán, *Chem. Mater.* **2013**, *25*, 1465; b) C. Vollmer, C. Janiak, *Coord. Chem. Rev.* **2011**, *255*, 2039.

[4] a) C. Vollmer, E. Redel, K. Abu-Shandi, R. Thomann, H. Manyar, C. Hardacre, C. Janiak, *Chem. Eur. J.* **2010**, *16*, 3849; b) E. Redel, R. Thomann, C. Janiak, *Chem. Commun.* **2008**, 1789; c) S. Peng, C. Wang, J. Xie, S. Sun, *J. Am. Chem. Soc.* **2006**, *128*, 10676; d) K. S. Suslick, M. Fang, T. Hyeon, *J. Am. Chem. Soc.* **1996**, *118*, 11960.

[5] C. Schöttle, P. Bockstaller, D. Gerthsen, C. Feldmann, *Chem. Commun.* **2014**, *50*, 4547; a) F. Gyger, P. Bockstaller, D. Gerthsen, C. Feldmann, *Angew. Chem. Int. Ed.* **2013**, *52*, 12443; *Angew. Chem.* **2013**, *125*, 12671; b) J. M. Yan, X. B. Zhang, S. Han, H. Shioyama, Q. Xu, *Angew. Chem. Int. Ed.* **2008**, *47*, 2287; *Angew. Chem.* **2008**, *120*, 2319; c) L. Xiong, T. He, *Chem. Mater.* **2006**, *18*, 2211; d) H. H. Nersisyan, J. H. Lee, C. W. Won, *Combust. Flame* **2005**, *142*, 241; e) Y.-H. Chang, H.-W. Wang, C.-W. Chiu, D.-S. Cheng, M.-Y. Yen, H.-T. Chiu, *Chem. Mater.* **2002**, *14*, 4334.

[6] a) A. Irzh, I. Genish, L. Klein, L. A. Solovyov, A. Gedanken, *Langmuir* **2010**, *26*, 5976; b) S. R. Ghanta, M. H. Rao, K. Muralidharan, *Dalton Trans.* **2013**, *42*, 8420; c) Y. Gao, J. Hao, *J. Phys. Chem. B* **2009**, *113*, 9461; d) F. Rataboul, C. Nayral, M.-J. Casanove, A. Maisonnat, B. Chaudret, *J. Organomet. Chem.* **2002**, *643*, 307.

[7] a) H. Braunschweig, R. D. Dewhurst, K. Hammond, J. Mies, K. Radacki, A. Vargas, *Science* **2012**, *336*, 1420; b) W. D. Woodul, E. Carter, R. Müller, A. F. Richards, A. Stasch, M. Kaupp, D. M. Murphy, M. Driess, C. Jones, *J. Am. Chem. Soc.* **2011**, *133*, 10074; c) K. Suzuki, T. Matsuo, D. Hashizume, H. Fueno, K. Tanaka, K. Tamao, *Science* **2011**, *331*, 1306; d) W. W. Brennessel, V. G. Young, J. E. Ellis, *Angew. Chem. Int. Ed.* **2006**, *45*, 7268; *Angew. Chem.* **2006**, *118*, 7426.

[8] Review: N. G. Connelly, W. E. Geiger, *Chem. Rev.* **1996**, *96*, 877.

[9] a) H. W. Chiu, C. N. Chervin, S. M. Kauzlarich, *Chem. Mater.* **2005**, *17*, 4858; b) A. L. Pickering, C. Mitterbauer, N. D. Browning, S. M. Kauzlarich, P. P. Power, *Chem. Commun.* **2007**, 580; c) R. K. Baldwin, K. A. Pettigrew, E. Ratai, M. P. Augustine, S. M. Kauzlarich, *Chem. Commun.* **2002**, 1822.

[10] a) B. M. Leonard, Q. Zhou, D. Wu, F. J. DiSalvo, *Chem. Mater.* **2011**, *23*, 1136; b) T. Ghosh, B. M. Leonard, Q. Zhou, F. J. DiSalvo, *Chem. Mater.* **2010**, *22*, 2190; c) G. Saravanan, H. Abe, Y. Xu, N. Sekido, H. Hirata, S. Matsumoto, H. Yoshikawa, Y. Yamabe-Mitarai, *Langmuir* **2010**, *26*, 11446; d) M. Schultz-Dobrick, S. K. Vijaya, M. Jansen, *J. Am. Chem. Soc.* **2005**, *127*, 12816.

[11] K. J. Jeon, H. R. Moon, A. M. Ruminski, B. Jiang, C. Kisielowski, R. Bardhan, J. J. Urban, *Nat. Mater.* **2011**, *10*, 286.

[12] a) D. V. Talapin, C. B. Murray, *Science* **2005**, *310*, 86; b) P. V. Nair, K. G. Thomas, *J. Phys. Chem. Lett.* **2010**, *1*, 2094.

[13] a) J. D. Benck, T. R. Hellstern, J. Kibsgaard, P. Chakthranont, T. F. Jaramillo, *ACS Catal.* **2014**, *4*, 3957; b) N. Huo, J. Kang, Z. Wei, S. S. Li, J. Li, S. H. Wei, *Adv. Funct. Mater.* **2014**, *24*, 7025; c) Y. Gong, S. Yang, L. Zhan, L. Ma, R. Vajtai, P. M. Ajayan, *Adv. Funct. Mater.* **2014**, *24*, 125.

[14] a) E. P. Rosenthal, E. F. Andrade, C. J. Arguello, R. M. Fernandes, L. Y. Xing, X. C. Wang, C. Q. Jin, A. J. Millis, A. N. Pasupathy, *Nat. Phys.* **2014**, *10*, 225; b) P. Liao, S. Lee, K. Esfarjani, G. Chen, *Phys. Rev. B* **2014**, *89*, 035108.

[15] a) T. Mitsudome, Y. Takahashi, T. Mizugaki, K. Jitsukawa, K. Kaneda, *Angew. Chem. Int. Ed.* **2014**, *53*, 8348; *Angew. Chem.* **2014**, *126*, 8488; b) J. Ohyama, T. Sato, Y. Yamamoto, S. Arai, A. Satsuma, *J. Am. Chem. Soc.* **2013**, *135*, 8016; c) M. Niu, Y. Wang, W. Li, J. Jiang, Z. Jin, *Catal. Commun.* **2013**, *38*, 77; d) X. Y. Quek, I. A. Filot, R. Pestman, R. A. van Santen, V. Petkov, E. J. Hensen, *Chem. Commun.* **2014**, *50*, 6005; e) J. Yi, J. T. Miller, D. Y. Zemlyanov, R. Zhang, P. J. Dietrich, F. H. Ribeiro, S. Suslov, M. M. Abu-Omar, *Angew. Chem. Int. Ed.* **2014**, *53*, 833; *Angew. Chem.* **2014**, *126*, 852.

[16] A. G. Knapton, *J. Inst. Met.* **1959**, *87*, 62.

Received: April 24, 2015
Published online: July 14, 2015

